Research

Estimation of current density distribution under electrodes for external defibrillation

Vessela Tz Krasteva* and Sava P Papazov

Address: Center for Biomedical Engineering, Bulgarian Academy of Sciences, Acad. G. Bonchev str. block 105 Sofia 1113, Bulgaria

Email: Vessela Tz Krasteva* - vessika@clbme.bas.bg; Sava P Papazov - papasow@vmei.acad.bg

* Corresponding author

Abstract

Background: Transthoracic defibrillation is the most common life-saving technique for the restoration of the heart rhythm of cardiac arrest victims. The procedure requires adequate application of large electrodes on the patient chest, to ensure low-resistance electrical contact. The current density distribution under the electrodes is non-uniform, leading to muscle contraction and pain, or risks of burning. The recent introduction of automatic external defibrillators and even wearable defibrillators, presents new demanding requirements for the structure of electrodes.

Method and Results: Using the pseudo-elliptic differential equation of Laplace type with appropriate boundary conditions and applying finite element method modeling, electrodes of various shapes and structure were studied. The non-uniformity of the current density distribution was shown to be moderately improved by adding a low resistivity layer between the metal and tissue and by a ring around the electrode perimeter. The inclusion of openings in long-term wearable electrodes additionally disturbs the current density profile. However, a number of small-size perforations may result in acceptable current density distribution.

Conclusion: The current density distribution non-uniformity of circular electrodes is about 30% less than that of square-shaped electrodes. The use of an interface layer of intermediate resistivity, comparable to that of the underlying tissues, and a high-resistivity perimeter ring, can further improve the distribution. The inclusion of skin aeration openings disturbs the current paths, but an appropriate selection of number and size provides a reasonable compromise.

Background

Defibrillation of the heart is widespread and well-established procedure for resuscitation of cardiac arrest victims [1]. The most accessible approach for electrical cardiac therapy is via external electrodes, placed on selected locations on the surface of the thorax. The electrodes have large contact area (70–120 cm^2) [2] and provide high and supposedly uniform current density distribution in the heart, needed for excitation of most myocardial cells, thus forcing them to return to normal rhythm. Many authors have investigated optimal electrode positions and sizes via two-dimensional (2D) [3,4] and three-dimensional (3D) [5–7] finite-element method (FEM) models, with the aim of obtaining uniform current distribution in the heart. The uniformity is evaluated by the ratio of the maximum current (which could result in myocardial damage) and the threshold current needed for defibrillation. For example Camacho et al. [5] found values of 2 to 4.7 for the anterior electrode position. Panescu et al. [6] reported that about 25% of the myocardium volume could be subjected to current densities more than 4 times higher than the threshold density.

Another aspect of the problem is the predominance of high current density along the perimeter of large size electrodes applied on human skin. In defibrillation and electrosurgery it can lead to unwanted damage and even severe skin burns [8–12] or electroporation [13], under the electrode perimeter area. In transthoracic pacing, it results in strong excitation of sensory nerve endings and provokes skeletal muscle contractions and pain [14,15].

To reduce these adverse effects, Wiley and Webster [8] suggested concentric segmented electrodes with higher resistance in the periphery, by the use of external resistors adjusted to equalise the currents in the separate segments. A similar approach has been considered in more detail by Kim and co-workers [14]. They have proposed covering the electrode metal with resistive gel of increasing resistivity toward the periphery, according to a specific relation with respect to the electrode radius. An implementation following such a design was tested on patients undergoing atrial cardioversion [16]. The skin damage after defibrillation was assessed by skin biopsy in selected points under the electrodes. The results showed less damage with the use of the modified electrodes compared to the standard ones. However, the authors noted that after separation of the cases where high energies and currents were applied, no difference was found in the skin damage data. This result was not explained. It might be due to breakdown of the higher resistivity electrode layer, or to the overall increase of the current density. Also, the skin resistivity and reaction to increased current density and temperature may very probably be nonlinear.

Another problem is related to skin irritation, resulting from long-term application of the electrodes, when a protective wearable defibrillator-monitor is used [17]. In such cases certain specific electrode designs were developed, providing openings for improvement of skin aeration or "breathing" [18].

The aim of the present work is to assess the current density distribution under electrodes of different structure, including shape, size, interfacing layer thickness and specific conductivity.

Method
The problem can be reduced to the solution of the pseudo-elliptic differential equation of Laplace type, provided the effects of quasi-stationarity are neglected.

$$\frac{\partial}{\partial x}\left(\frac{1}{\rho}\frac{\partial V}{\partial x}\right) + \frac{\partial}{\partial y}\left(\frac{1}{\rho}\frac{\partial V}{\partial y}\right) + \frac{\partial}{\partial z}\left(\frac{1}{\rho}\frac{\partial V}{\partial z}\right) = 0. \qquad (1)$$

The solution can be obtained for the scalar electrical potential *V* in an electrically conductive domain consisting of layers of different specific resistivity ρ. The equation is solved subject to the following boundary conditions:

- Dirichlet boundary conditions imposed on the surface SEi in contact with the ith electrode at potential Vi:

$$V\left(x,y,z\right)\big|_{SE_i} = V_i. \qquad (2)$$

- Neumann boundary conditions state that the normal component of the derivative of the potential is zero in the remaining boundary plane (SB), not in contact with the electrodes:

$$\left(\frac{\partial V\left(x,y,z\right)}{\partial n}\right)_{SB} = 0. \qquad (3)$$

The current density distribution is defined by the potential gradient and the specific conductivity σ of the different regions:

$$J(x,y,z) = \sigma\left(-gradV(x,y,z)\right), \qquad (4)$$

here $\sigma = \dfrac{1}{\rho}$.

In this case, the propagation of the low frequency electromagnetic field is virtually free of the feedback action from eddy currents, as the human tissue is weakly conductive. Therefore, the skin effect can be neglected.

In this study, the finite element method (FEM) was used to estimate the current density distribution in a partially homogeneous conductive medium. It consists of homogeneous layers (Fig. 1a), simulating the electrode metal, the electrode-skin interface and part of a human body. All structures are modeled as purely resistive, as it has been shown that in defibrillation there was no phase difference between applied voltage and current passed through the thorax [19,20].

Using software for FEM modelling and 3D-computer graphics (parts of ANSYS 5.7 and MATLAB 5.2), a simplified 3D finite element model with over 50,000 eight-node tetrahedron elements was developed (Fig. 1b). Since the measurements were taken 0.5 mm under the electrode-skin interface, the geometry of the thorax was simplified and simulated as a cylindrical domain (10 cm radius; 10 cm height), with specific resistivity 20 Ω*m*. This value was chosen as an approximate average of very high and very low conductivities (soft tissue, blood and bone, lung air). The estimated inter-electrode resistance $R \approx \rho\,l/S \approx 65\Omega$ (*l* – distance between the electrodes, *S* – electrode surface),
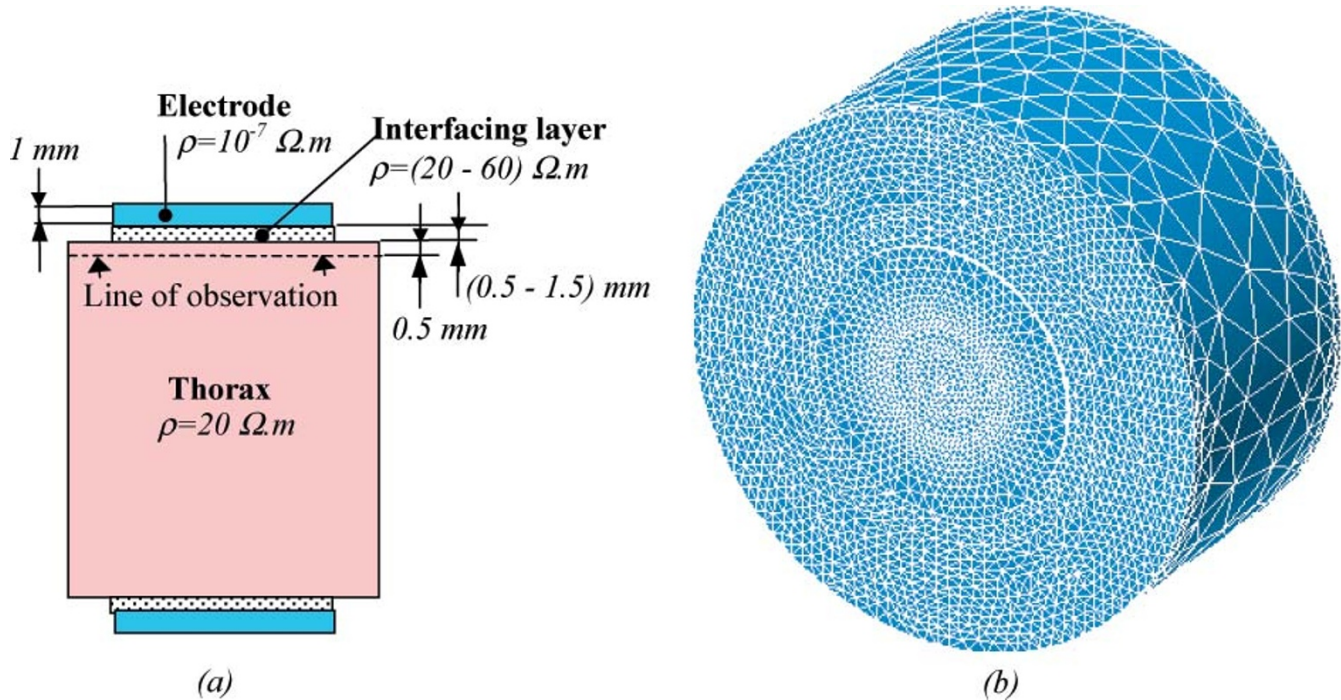
Figure 1
Model of electrode-tissue contact. (a) Disposition of the electrodes (cross-section). (b) Finite-element model with over 50,000 elements.

corresponds to the real conditions in defibrillation. The electrodes, of about 80 cm² area and 1 mm thickness, were located on the surface of the upper and lower cylinder bases. The defibrillation voltage was applied on the group of nodes forming the exterior electrode surface. The inter-electrode potential difference used in all comparative studies was set at 1000 V. This value was selected for convenience, since the relative distribution is independent of the voltage applied. The interfacing gel was simulated by a thick (0.5 – 1.5 mm) low-resistivity (20 – 60 Ωm) layer under the electrodes. Thus a varying layer resistance was represented, in a range of 1.5% to 15% of the total thoracic resistance, i.e. value from 1 to 10 Ω.

Results
Standard electrode configurations
The results of the current distribution simulation, obtained for a plane at 0.5 mm under the most commonly used electrode types – rectangular or square-shaped and circular, is presented in Fig. 2a and 2b respectively. The current density profiles along selected axes are shown at the right side. The interfacing layer, of equal surface with the electrode, was chosen of 20 Ωm specific resistivity and 0.5 mm thickness. Thus the total interface resistance under both electrodes did not exceed 2.5 Ω. The square-

shaped (8.86 cm side) and circular (5 cm radius) electrodes were of equal 80 cm² area.

Circular electrode analysis
Circular electrodes of different sizes were compared. Two types of electrodes were designed: one of 5 cm and another of 2.5 cm radius. The respective current density distributions are shown in Fig. 3. The interfacing layer resistivity in both configurations was varied to obtain equal non-uniformity, assessed by the so called "non-uniformity coefficient". The latter was chosen as the ratio (K) of the maximum to the minimum current density: K=Jmax/Jmin. The respective results are presented in Table 1.

In an attempt to obtain more uniform current distribution, a ring (2 mm width) of higher specific resistivity (ρ = 100 Ωm) was added to the interface perimeter, with a thin isolating barrier between the layer under the electrode and the ring (Fig. 4). Thus the peak current density decreased from 1780 A/m² (1 – without ring) to 1570 A/m² (2 – with ring).

The influence of the interfacing layer thickness and specific resistivity ρ was examined by using an electrode of con-
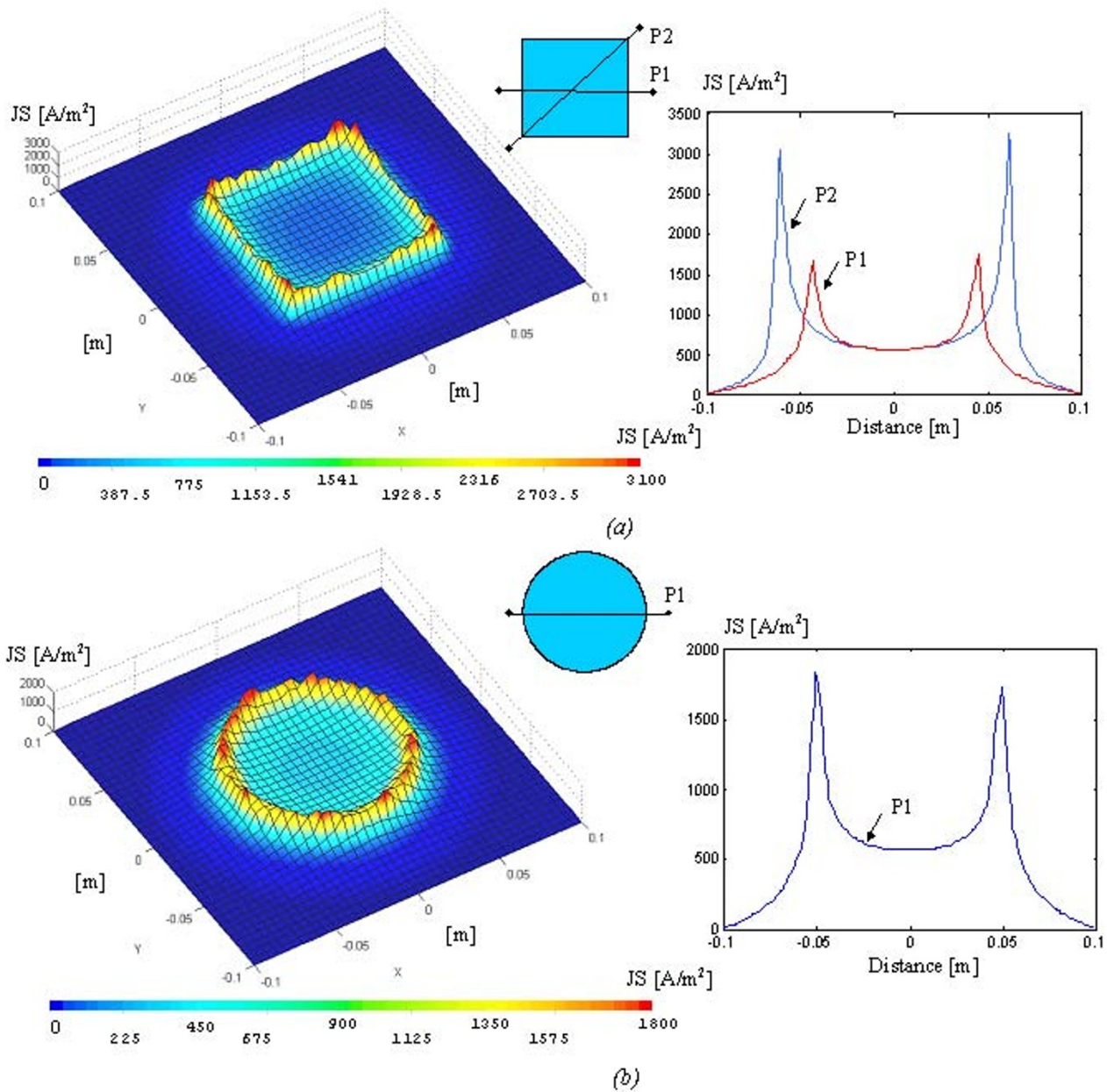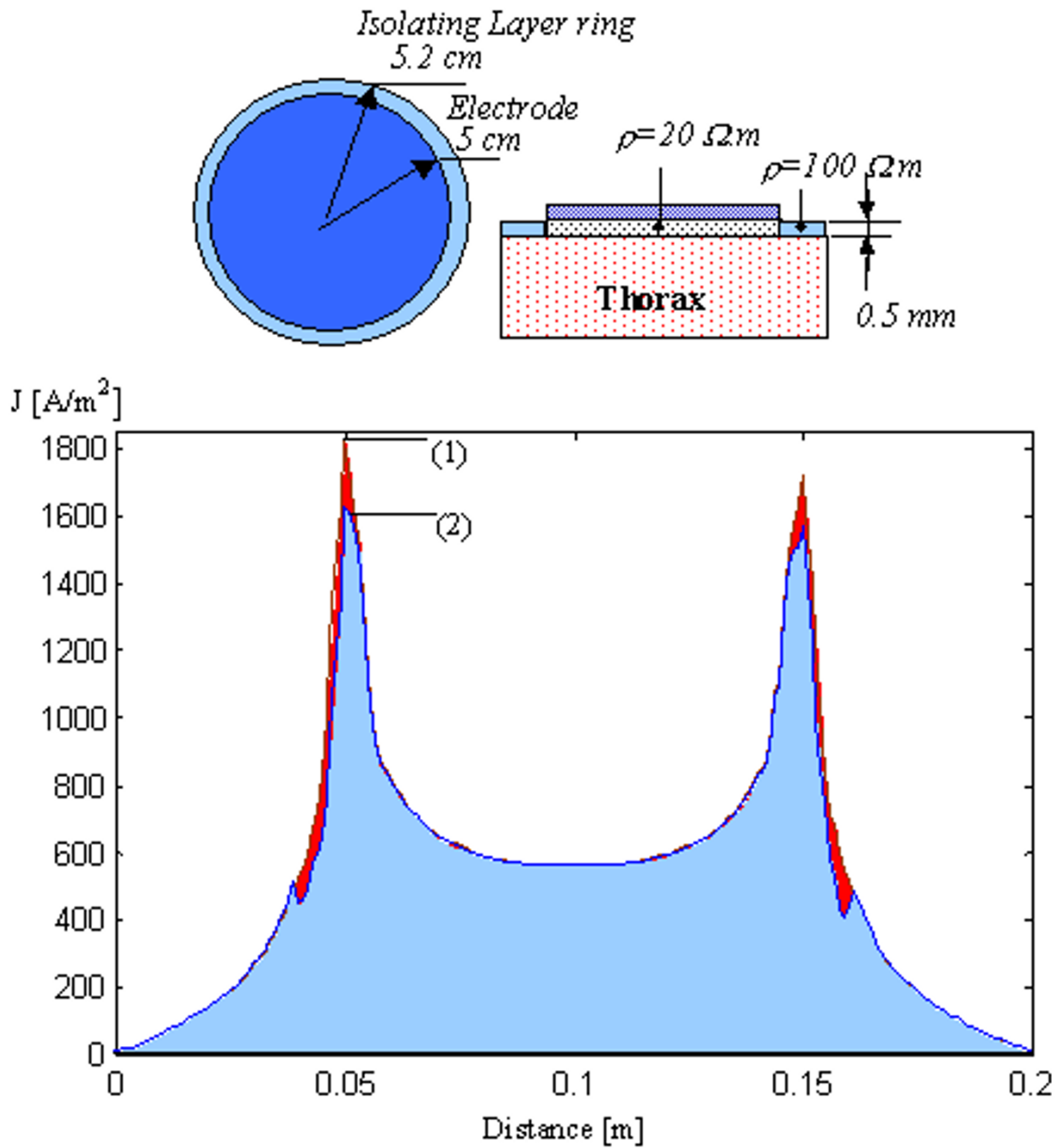
Figure 2
Current density distribution profiles in a plane parallel to the electrode and 0.5 mm under the interface layer. Right-side graphs – current density along selected axes in this plane. (a) square-shaped electrode (8.86 cm side), area ~80 cm^2; (b) circular electrode (5 cm radius), area ~80 cm^2.
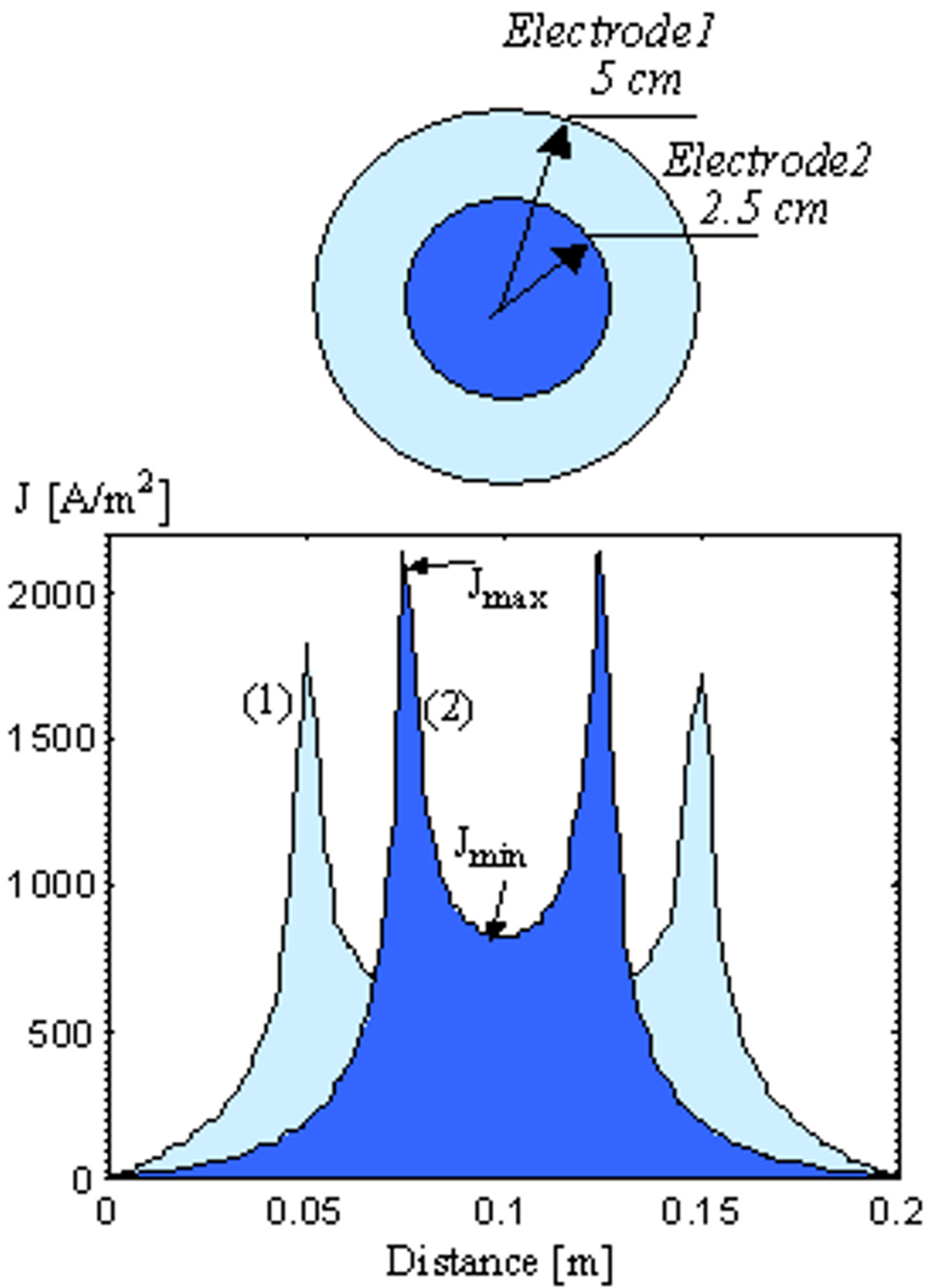
Figure 3
Current density distribution profiles under two circular electrodes. (1) 5 cm radius; (2) 2.5 cm radius.
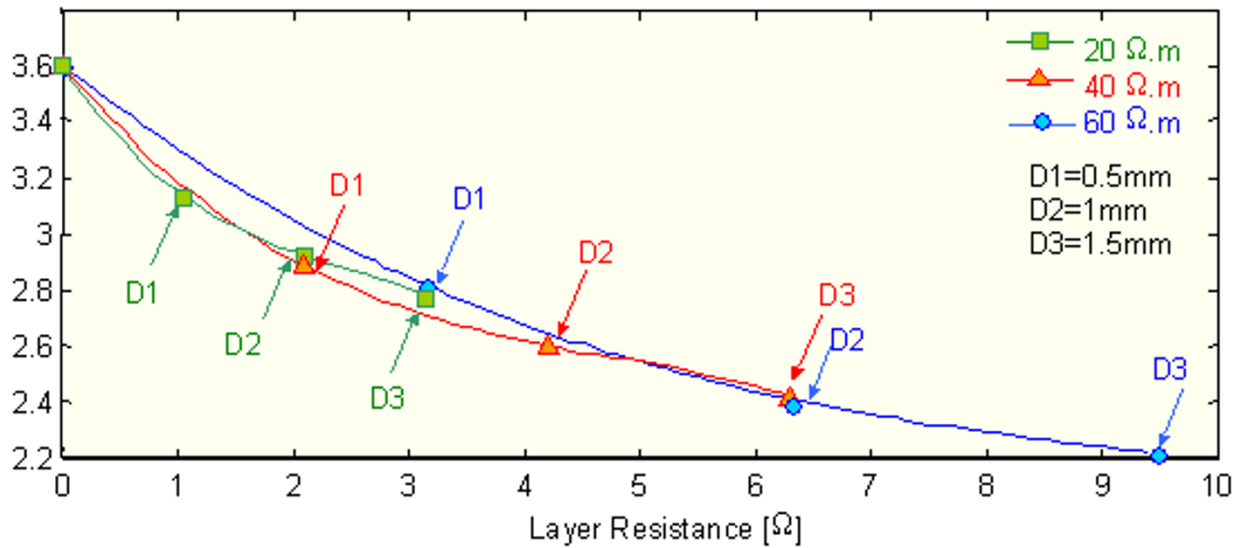
Figure 4
Current density distribution profiles under circular electrodes. Comparison between (1) r = 5 cm and (2) r = 5 cm and an additional surrounding ring solidified layer with ρ = 100 Ωm.

Table 1: Comparative results for two electrodes with different radii.

Electrode Radius [*cm*]	Interfacing layer (5 mm thickness)		Jmax/Jmin [*Am*$^{-2}$]	K=Jmax/Jmin
	ρ [Ω*m*]	R [Ω]		
5	20	**1.25**	1780/570	**3.12**
2.5	4	**1.25**	2450/800	**3.06**
5	80	**5.1**	1490/550	**2.71**
2.5	20	**5.1**	2150/780	**2.76**

Figure 5
Effect of current density non-uniformity coefficient K of resistance layers with different thickness (D1 = 0.5 mm, D2 = 1.0 mm, D3 = 1.5 mm) and specific resistivity (ρ = 20, 40, 60 Ω*m*).

stant radius (5 cm) and variable gel characteristics. Nine simulations were performed: three for ρ = 20 Ω*m* (interface thickness 0.5, 1.0 and 1.5 mm), and three each for ρ = 40 Ω*m* and ρ = 60 Ω*m*, respectively. The results for the estimated "non-uniformity" coefficient K as a function of the overall electrode-interface resistance are presented in Fig. 5.

The current density distribution in a plane perpendicular to the circular electrode surface is shown in Fig. 6a. The peak densities at the electrodes periphery decrease relatively rapidly with depth in the 'thorax' domain. To better observe this effect, several detailed profiles are taken along the dotted axes, marked in the vertical-section plane, at

0.5, 10, 20 and 50 mm depth under the interfacing layer surface (Fig. 6b).

Various electrode configurations
Electrodes of various shapes were designed, presumably more suitable for long-term wearing. Their respective shape and distribution profiles are shown in Figs. 7,8,9,10,11. The electrodes of Fig. 7, 10 and 11 are circular (5 cm radius; 0.5 mm interface layer thickness; ρ = 20 Ω*m*) with openings for improvement of skin aeration. We also simulated an electrode where the openings were replaced by conductive elements (Fig. 8). The four circular electrodes in Fig. 9, each surrounded by an additional ring, are of the same total area as the 5 cm radius circular electrode
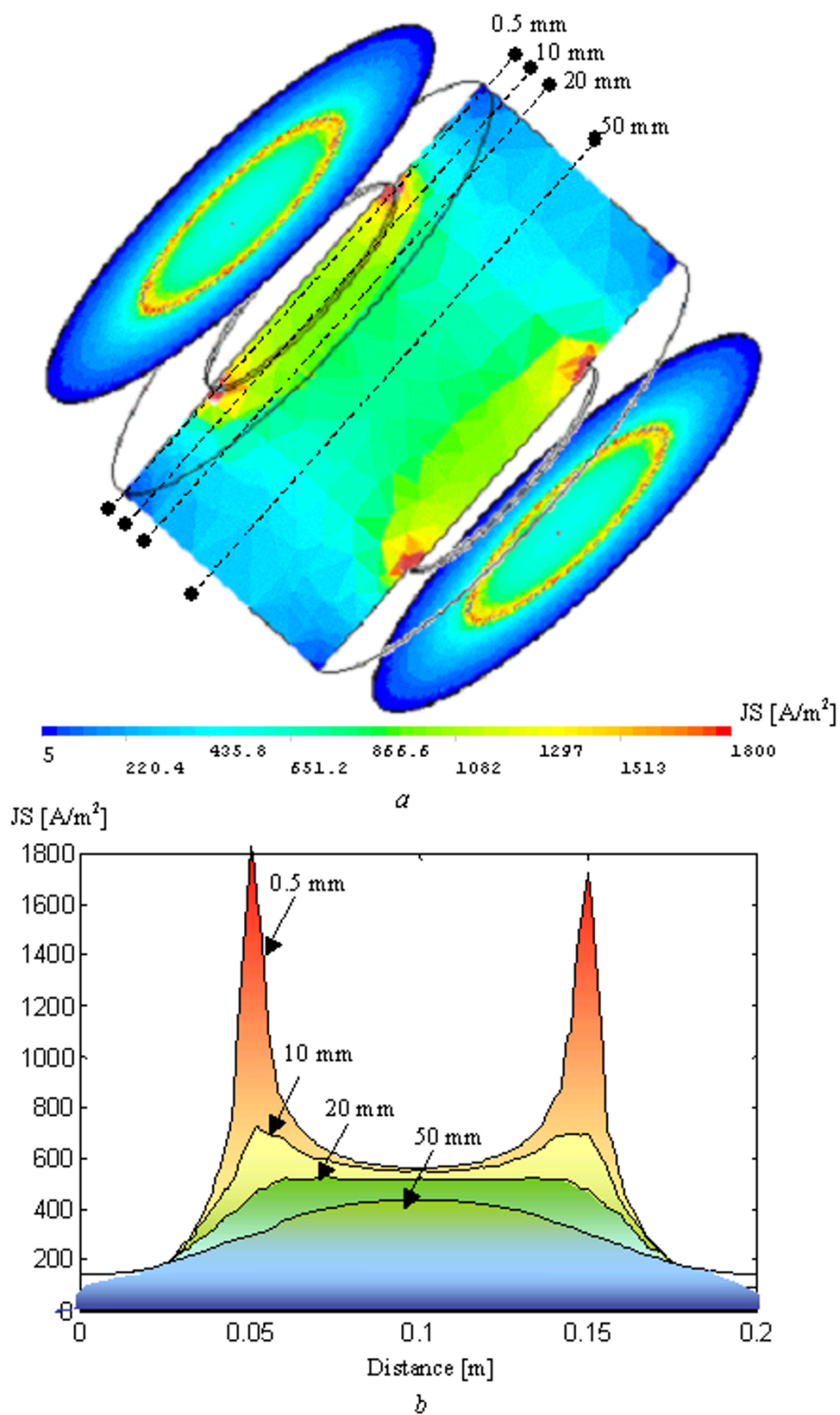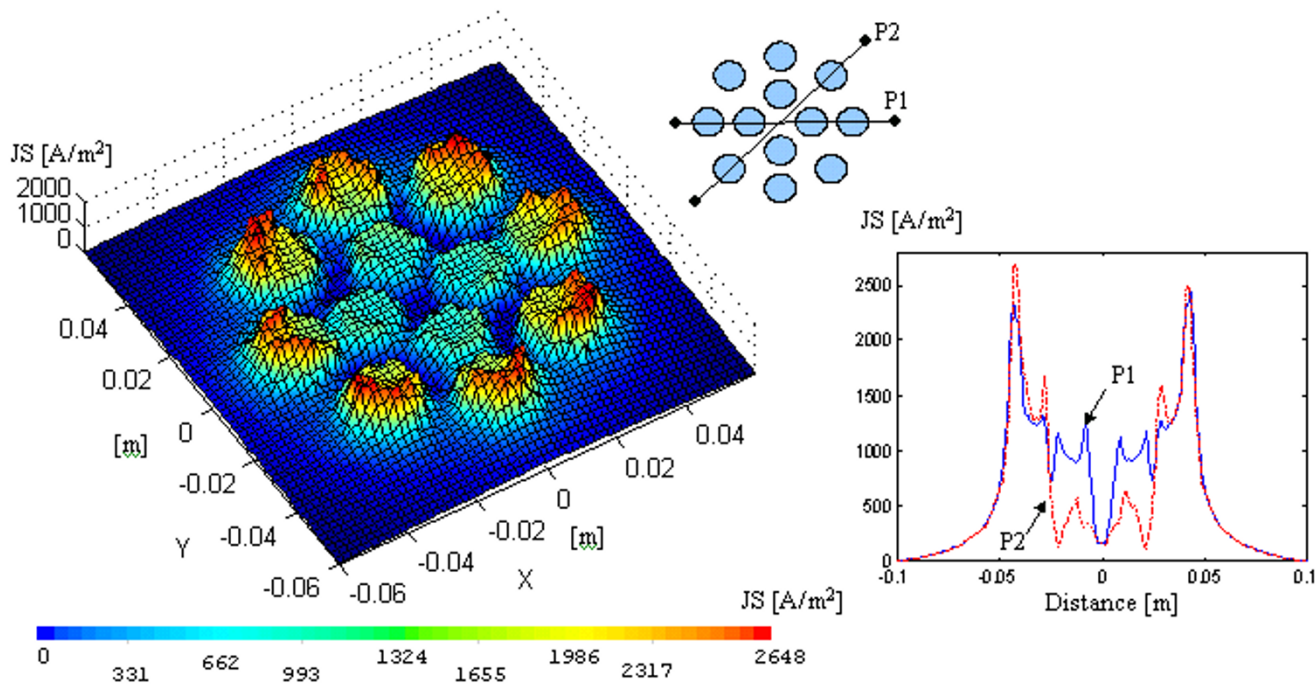
Figure 6
Current density profile taken: (a) in a plane perpendicular to the electrode surface; (b) more detailed profiles along the dotted axes, marked in the vertical-section plane, at 0.5, 10, 20 and 50 mm depth.
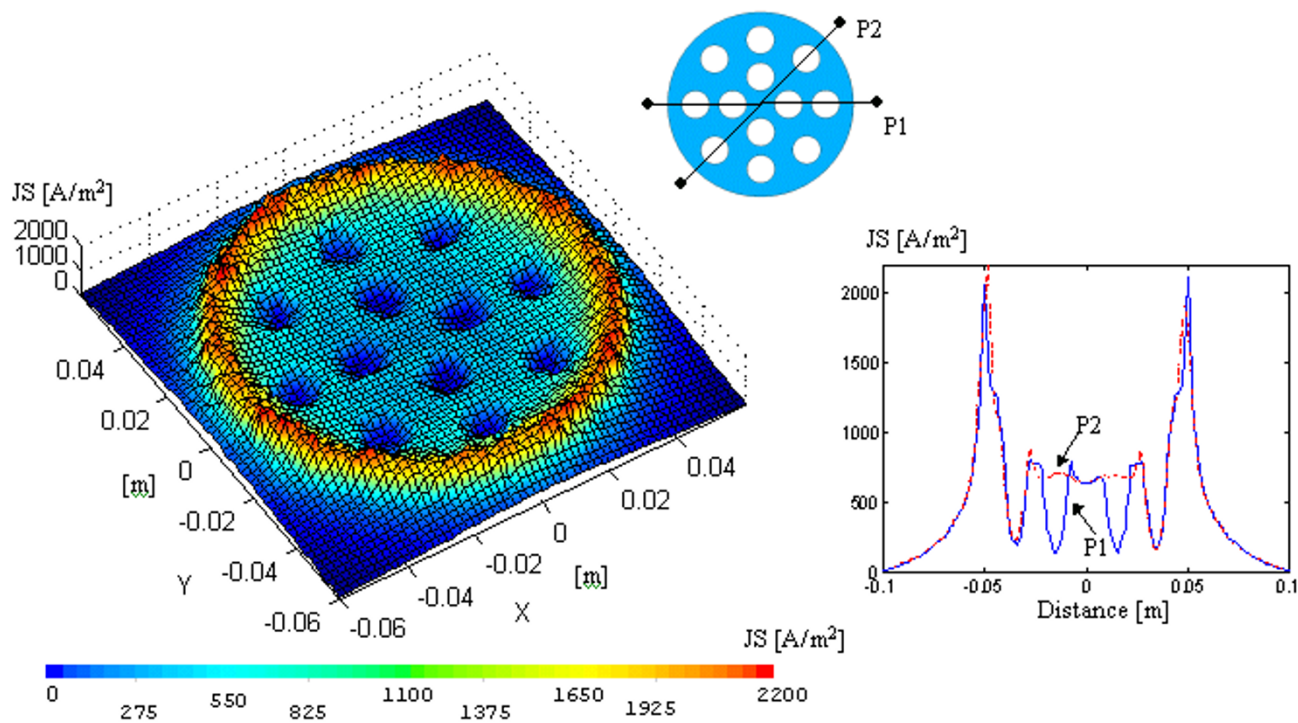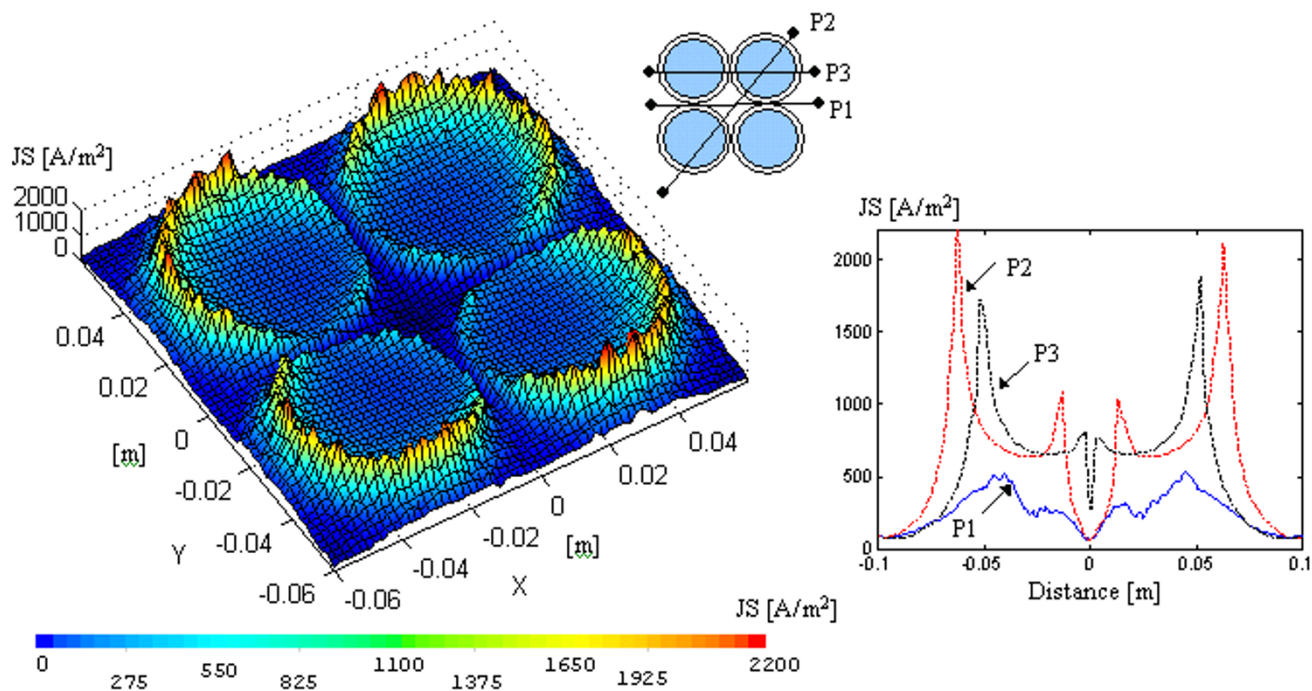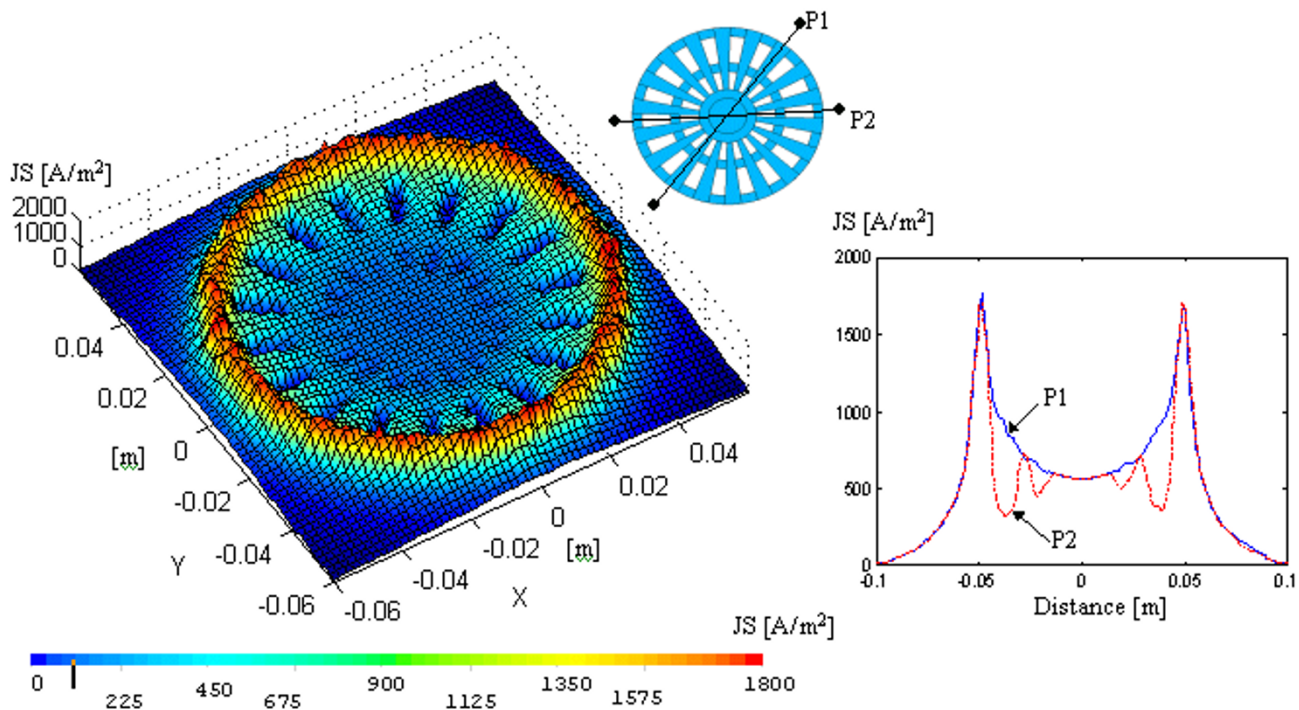
Figure 7
Current density distribution for a circular electrode with aeration openings. Right-side graphs – profiles along selected axes.
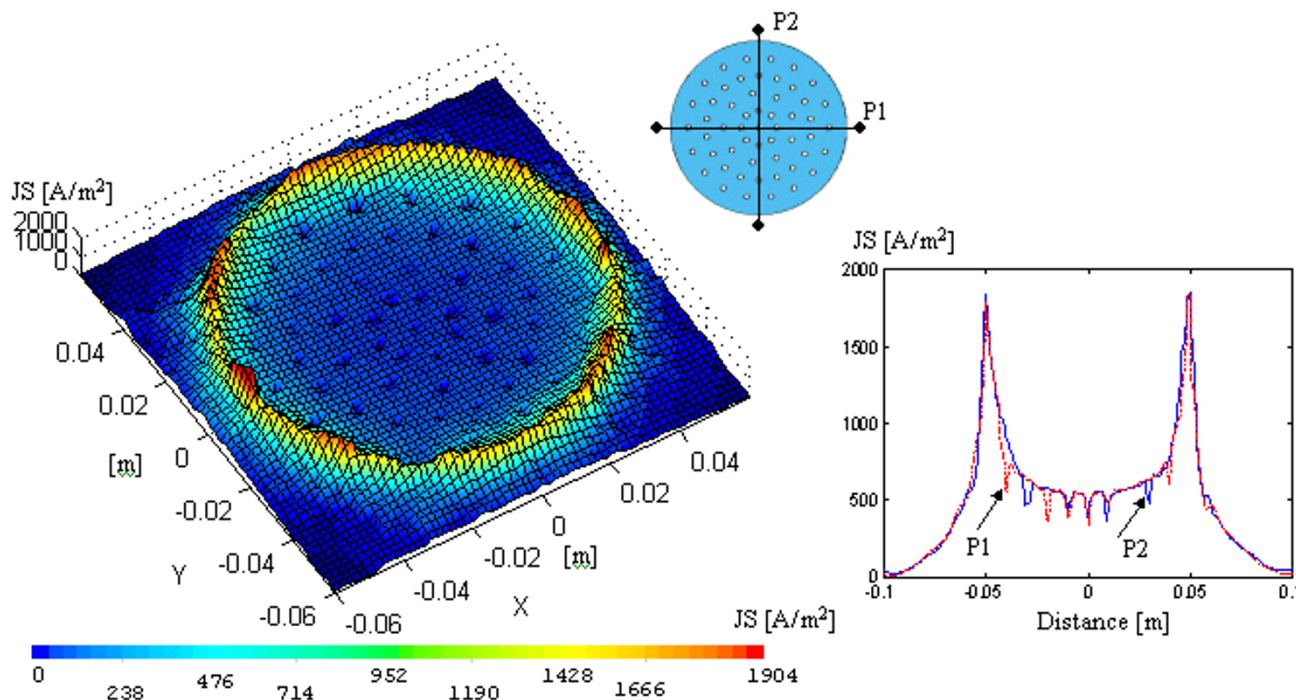

Figure 8
Current density distribution for a multi-disk electrode. Right-side graphs – profiles along selected axes.

Figure 9
Current density distribution for a four-disk electrode with additional high-resistivity rings. Right-side graphs – profiles along selected axes.

Figure 10
Current density distribution for a circular electrode with sector-shaped aeration openings. Right-side graphs – profiles along selected axes.

Figure 11
Current density distribution for a circular electrode with small aeration openings. Right-side graphs – profiles along selected axes.

of Fig. 4. The "non-uniformity" coefficient of the current density distribution profile reaches very high values (K > 11) in a plane 0.5 mm below the interfacing gel. The performance of each electrode configuration was assessed also by the current distribution profile along an axis in the central region, at 50 mm depth in the 'thorax' domain (Fig. 12).

Discussion

Commonly used rectangular electrodes (area ~80 cm^2) exhibit high non-uniformity of the current density distribution at the electrode-skin interface. The profile across the corners shows a non-uniformity coefficient of 4.6 (Fig. 2a). The standard circular electrode with the same area yields 32% lower non-uniformity (Fig. 2b).

Smaller electrodes produce higher current density, with slightly lower non-uniformity (Fig. 3). However, the electrode radius cannot be less than 4.7 cm for the minimum area of 70 cm^2, recommended for efficient defibrillation.

The resistance of the electrode-skin interfacing layer is a major determinant of the maximum current density in the distribution profile. Two electrodes with different radii show equal non-uniformity, assessed by the coefficient K=

Jmax/Jmin, if the under-electrode layer specific resistivity is chosen to provide the same electrode resistance (Table 1). This result was confirmed also for interfacing layers of different thicknesses (Fig. 5). For example, a thick layer with lower specific resistance ($\rho = 20\ \Omega m$ and 1.5 mm thickness) has the same performance as a thin layer with higher ρ ($\rho = 60\ \Omega m$ and 0.5 mm thickness). This result did not confirm our expectations that the thickness of the interface has a certain straightening effect on the current lines. A higher layer resistance is associated with lower non-uniformity, but it should not add more than 3–5% to the total resistance of the defibrillation current path. Many authors investigated the advantage of covering the electrode metal with resistive layers of increasing resistivity toward the periphery [14,21]. Such a technique seems technologically difficult and expensive for disposable electrodes. The use of a ring of higher resistivity along the electrode perimeter seems acceptable, as the resistance in the current pathway was not increased, the maximum periphery current was reduced by 12% and the non-uniformity coefficient dropped to K = 2.71 (1570/580 A/m^2). The same result could be achieved with 3 times higher resistance of a uniform layer. However, the problem of technological difficulties remains open.
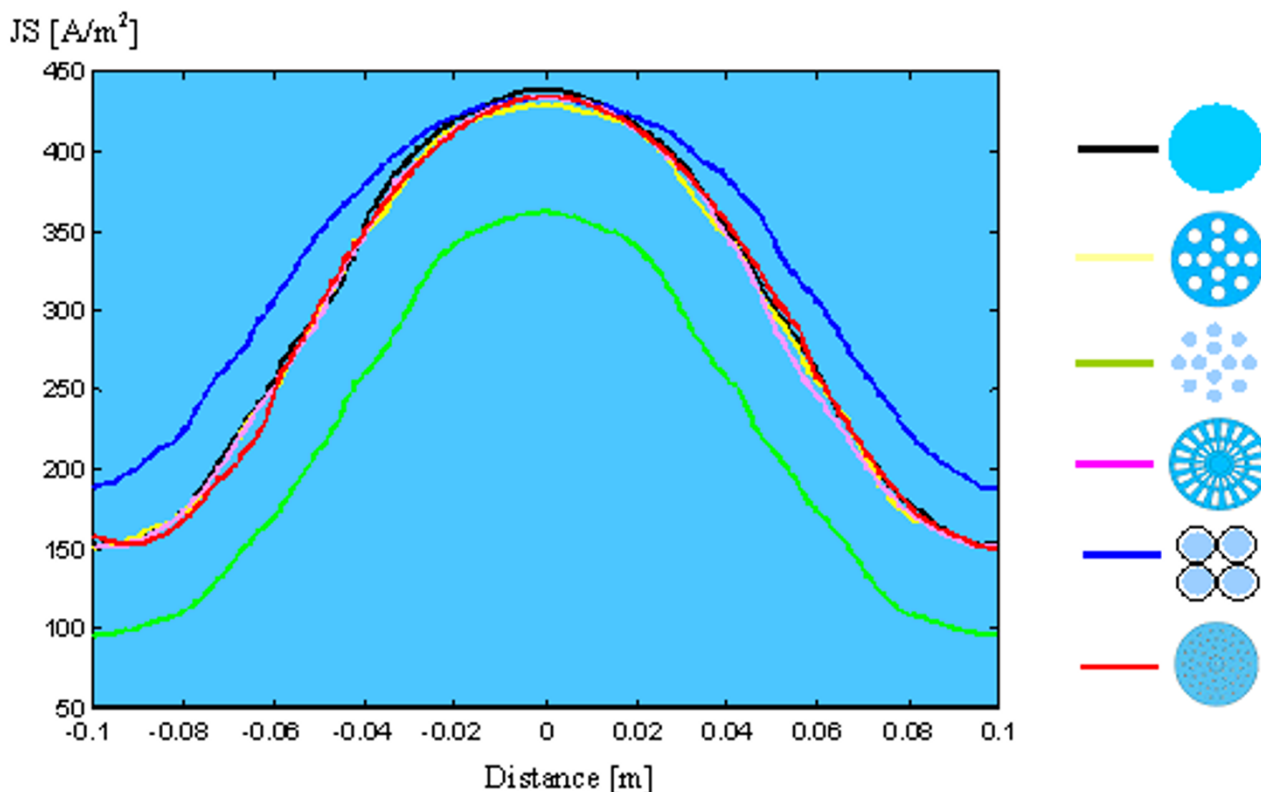
Figure 12
Current density profiles for different electrodes at 50 mm depth along the respective dotted axis, marked in the vertical-section plane of Fig. 6a.

Various electrode structures with openings for skin "breathing" (Figs. 7,8,9,10,11), increase the effect of non-uniformity, as the current density under the vents drops strongly. However, the distribution non-uniformity becomes negligible with increased distance from the electrode surface, as evident in Fig. 6. The bell-shaped distribution in Fig. 12 is estimated for the central region of the cylindrical thorax model, 50 mm under the interfacing layer surface. Consequently, the current density distribution under various electrode structures relates to effects on the skin, rather than to the defibrillation efficiency.

Conclusion
The current density distribution non-uniformity of circular electrodes is about 30% smaller than that of square-shaped electrodes. The use of an interface layer of intermediate resistivity, comparable to that of the underlying tissues can further improve the distribution. A high-resistivity perimeter ring adds a further 13% improvement without increasing the total interface resistance, hence the

resistance to the defibrillation current, which is an important advantage in defibrillation.

The inclusion of skin aeration openings for wearable electrodes disturbs the current paths, but an appropriate selection of number and size provides a reasonable compromise.

Authors' contributions
VTK solved the problems of adequate FEM modeling, the development of various electrode configurations, and generation and presentation of the current distribution profiles. SPP was responsible for the theoretical basis of the investigation and for the setting the main ideas in the solution analysis. Both authors read and approved the final manuscript.

Acknowledgements

References

1. International Liaison Committee on Resuscitation **Guidelines 2000 for Cardiopulmonary Resuscitation and Emergency Cardiovascular Care.** *Circulation* 2000, **102:**I86-90
2. Geddes LA **Electrodes for transchest and ICD defibrillation and multifunctional electrodes.** *In: Defibrillation of the heart. ICDs, AEDs and Manual (Edited by: Tacker WA) Mosby, St Louis* 1994, 82-118
3. Fahy BJ **Optimal electrode configurations for external cardiac pacing and defibrillation: an inhomogeneous study.** *IEEE Transactions on Biomedical Engineering* 1987, **34:**743-748
4. Lehr JL, Ramirez IF, Karlon WJ and Eisenberg SR **Test of four defibrillation dosing strategies using a two-dimensional finite-element model.** *Medical & Biological Engineering & Computing* 1992, **30:**621-628
5. Camacho MA, Lehr JL and Eisenberg WJ **A three-dimensional finite element model of human transthoracic defibrillation: paddle placement and size.** *IEEE Transactions on Biomedical Engineering* 1995, **42:**572-578
6. Panescu D, Webster JG, Tompkins WJ and Stratbrucker RA **Optimization of cardiac defibrillation by three dimensional finite element modelling of the human thorax.** *IEEE Transactions on Biomedical Engineering* 1995, **42:**185-191
7. Jorgenson DB, Haynor DR, Bardy GH and Kim Y **Computational studies of transthoracic and transvenous defibrillation in a detailed 3D human thorax model.** *IEEE Transactions on Biomedical Engineering* 1995, **42:**172-183
8. Wiley JD and Webster JG **Analysis and control of the current distribution under circular dispersive electrodes.** *IEEE Transactions on Biomedical Engineering* 1982, **29:**381-385
9. Wiley JD and Webster JG **Distributed equivalent-circuit model for circular dispersive electrodes.** *IEEE Transactions on Biomedical Engineering* 1982, **29:**385-389
10. McNaughton GW, Wyatt JP and Byrne JC **Defibrillation – a burning issue in coronary care units.** *Scottish Medical Journal* 1996, **41:**47-48
11. Battig CG **Electrosurgical burns and their prevention.** *JAMA* 1968, **204:**1025-1029
12. Pagan-Carlo LA, Stone MS and Kerber RE **Nature and determinants of skin 'burns' after transthoracic cardioversion.** *Am J Cardiology* 1997, **79:**689-691
13. Vogel U, Wanner T and Bultmann B **Extensive pectoral muscle necrosis after defibrillation: nonthermal skeletal muscle damage caused by electroporation.** *Intensive Care Medicine* 1998, **24:**743-745
14. Kim Y and Schimpf PH **Electrical behavior of defibrillation and pacing electrodes.** *Proceedings of the IEEE* 1996, **84:**446-456
15. Birkui PJ, Trigano LA, Zoll PM and eds **Noninvasive transcutaneous cardiac pacing.** *Futura Publ Inc Mount Kisco, New York* 1992, 179-191
16. Garcia LA, Pagan-Carlo LA, Stone MS and Kerber RE **High perimeter impedance defibrillation electrodes reduce skin burns in transthoracic cardioversion.** *American Journal of Cardiology* 1998, **82:**1125-1127
17. Schott R **Wearable defibrillator.** *Cardiovasc J Nurs* 2002, **16:**44-52
18. Totman M, O'Leary J, Owen JM and Fincke RW **Defibrillation system.** *US Patent No 6374138* 2002,
19. Tacker WA and Geddes LA **The laws of electrical stimulation of cardiac tissue.** *Proceedings of the IEEE* 1996, **84:**355-65
20. Al Hatib F, Trendafilova E and Daskalov I **Thransthoracic electrical impedance during external defibrillation: comparison of measured and modeled waveforms.** *Physiological Measurement* 2000, **21:**145-153
21. Papazov S, Kostov Z and Daskalov I **Electrical current distribution under transthoracic defibrillation and pacing electrodes.** *J Med Eng & Technol* 2002, **26:**22-27